Synthesis and Characterization of Ruthenium(II) Molecular Assemblies for Photosensitization of Nanocrystalline TiO_2: Utilization of Hydroxyl Grafting Mode

Bobak Gholamkhass, Kazuhide Koike,* Nobuaki Negishi, Hisao Hori, and Koji Takeuchi

Global Warming Control Department, National Institute for Resources and Environment, 16-3 Onogawa, Tsukuba, Ibaraki, 305 Japan

Received June 19, 2000

New Ru polypyridine complexes $[(bpy)_2Ru(L)]^{2+}$, where bpy = 2,2′-bipyridine and L = dipyrido[3,2-*a*:2′,3′-*c*]-phenazine-2-carboxylic acid (dppzc), dipyrido[3,2-*f*:2′,3′-*h*]quinoxaline-2,3-dicarboxylic acid (dpq$(COOH)_2$), 3-hydroxydipyrido[3,2-*f*:2′,3′-*h*]quinoxaline-2-carboxylic acid (dpq(OHCOOH)), 2,3-dihydroxydipyrido[3,2-*f*:2′,3′-*h*]quinoxaline (dpq$(OH)_2$), and $[(L')Ru(dppzc)_2]^{2+}$, where L′ = bpy and 1,10-phenanthroline (phen), have been synthesized, characterized, and anchored to nanocrystalline TiO_2 electrodes for light to electrical energy conversion in regenerative photoelectrochemical cells with I^-/I_2 acetonitrile electrolyte. These sensitizers have intense metal-to-ligand charge-transfer (MLCT) bands centered at ∼450 nm. The effect of pH on the absorption and emission spectra of these complexes consisting of protonatable ligands has been investigated in water by spectrophotometric titration. The excited-state pK_a values are more basic than the ground-state ones, except the pK_{a2} and pK_{a2}* in $[(bpy)_2Ru(dpq(OH)_2)]^{2+}$, which are equal, suggesting the localization of the lowest-energy MLCT on heteroaromatic bridging ligands, dppzc and dpq. Incident photon-to-current conversion efficiency (IPCE) is sensitive to the structural changes that resulted from introducing different functional groups, used for grafting.

Introduction

Titanium dioxide is a semiconductor with a wide band gap that has been demonstrated to be a promising material for the production of regenerative solar cells.[1,2] The major reason for its wide application is the large surface-to-volume ratio of the nanocrystalline TiO_2. Consequently, a large number of dye molecules can be adsorbed onto its surface and even a monolayer of the dye adsorbed on the electrode will absorb enough energy from the incident light photons to give a high yield of conversion. Using a variety of organic[1] and inorganic[2] dyes, the photosensitivity of TiO_2 can be extended to the visible region (λ > 400 nm) of solar irradiation. This dye is the most important element of the solar cell because the dye molecule injects an electron into the conduction band of the semiconductor following the production of its excited state upon light absorption.[3] Among inorganic dyes, particularly, ruthenium complexes are widely used because of the intense absorption in the visible range of the spectra, excellent photochemical stability, and strong emissive character.[4] Another important factor which makes Ru a viable choice is the ability to introduce ligands with delicate characteristics into its octahedral geometry.[5] In fact, ligands which bridge the metal center to the acceptor site of the semiconductor in such systems play an important role. This is because, first, the bridging ligand dictates the whole structure and directionality of the donor−acceptor system; second, with its coordinating sites it contributes to determine the spectroscopic and redox properties of metal-based units; and third, it controls the electronic communication between the electron donor (D) and acceptor (A). Therefore, the selection of suitable bridging ligands is crucial to obtain a well-designed photoactive device.

A significant body of research currently exploits the synthesis of photoactive ruthenium compounds, for the study of their photochemical, photophysical, and electrochemical properties. These investigations have attempted to design and construct new ligands and their corresponding ruthenium complexes capable of performing useful light-induced functions.[5] In these Ru complexes, a metal-to-ligand charge-transfer (MLCT) state of the Ru(II) moiety, (^{3}CT)Ru, is responsible for all its photochemistry. In the cases where the Ru compound is adsorbed on the semiconductor surface for the sensitization to visible light, the decay of the (^{3}CT)Ru excited state was accelerated by electron injection into the semiconductor conduction band.[3]

(1) See, for example: (a) Moser, J. E.; Grätzel, M. *Chem. Phys.* **1993**, *176*, 493. (b) Li, D.-Q.; Swanson, B. I.; Robinson, J. M.; Hoffbauer, M. A. *J. Am. Chem. Soc.* **1993**, *115*, 6975. (c) Marguerettaz, X.; Fitzmaurice, D. *J. Am. Chem. Soc.* **1994**, *116*, 5017. (d) Spitler, M. T.; Calvin, M. *J. Chem. Phys.* **1977**, *66* (10), 4294.

(2) (a) Weller, H.; Eychmuller, A. *Adv.Photochem.* **1998**, *20*, 165 and references therein. (b) O'Regan, B.; Grätzel, M. *Nature* **1991**, *353*, 737. (c) Argazzi, R.; Bignozzi, C. A.; Hasselmann, G. M.; Meyer, G. J. *Inorg. Chem.* **1998**, *37*, 4533.

(3) Tachibana, Y.; Moser, J. E.; Gratzel, M.; Klug, D. R.; Durrant, J. R. *J. Phys. Chem.* **1996**, *100*, 20056.

(4) (a) Juris, A.; Balzani, V.; Barigelletti, F.; Campagna, S.; Belser, P.; von Zelewsky, A. *Coord. Chem. Rev.* **1988**, *84*, 85. (b) Balzani, V.; Juris, A.; Venturi, M.; Campagna, S.; Serroni, S. *Chem. Rev.* **1996**, *96*, 759 and references therein. (c) Mesmaeker, A. K.-D.; Lecomte, J.-P.; Kelly, J. M. *Top. Curr. Chem.* **1996**, *177*, 25. (d) Balzani, V.; Scandola, F. In *Comprehensive Supramolecular Photochemistry;* Atwood, J., MacNicol, D., Davies, E., Vogtle, F., Lehn, J.-M., Eds.; Pergamon Press: Oxford, U.K., 1996; Vol. 10, p 687.

(5) (a) Zakeeruddin, S. M.; Nazeeruddin, Md. K.; Humphry-Baker, R.; Grätzel, M. *Inorg. Chem.* **1998**, *37*, 5251. (b) Bolger, J.; Gourdon, A.; Ishow, E.; Launay, J.-P. *Inorg. Chem.* **1996**, *35*, 2937. (c) Balzani, V.; Barigelletti, F.; Belser, P.; Bernhard, S.; De Cola, L.; Flamigni, L. *J. Phys. Chem.* **1996**, *100*, 16786. (d) Gourdon, A.; Launay, J.-P. *Inorg. Chem.* **1998**, *37*, 5336. (e) Kajita, T.; Leasure, R. M.; Devenney, M.; Friesen, D.; Meyer, T. J. *Inorg. Chem.* **1998**, *37*, 4782. (f) Moucheron, C.; Mesmaeker, A. K.-D.; Choua, S. *Inorg. Chem.* **1997**, *36*, 584. (g) Indelli, M. T.; Bignozzi, C. A.; Scandola, F.; Collin, J.-P. *Inorg. Chem.* **1998**, *37*, 6084. (h) Hartshorn, R. M.; Barton, J. K. *J. Am. Chem. Soc.* **1992**, *114*, 5919. (i) Collin, J.-P.; Gavina, P.; Heitz, V.; Sauvage, J.-P. *Eur. J. Inorg. Chem.* **1998**, 1.

10.1021/ic0006605 CCC: $20.00
Published on Web 01/09/2001

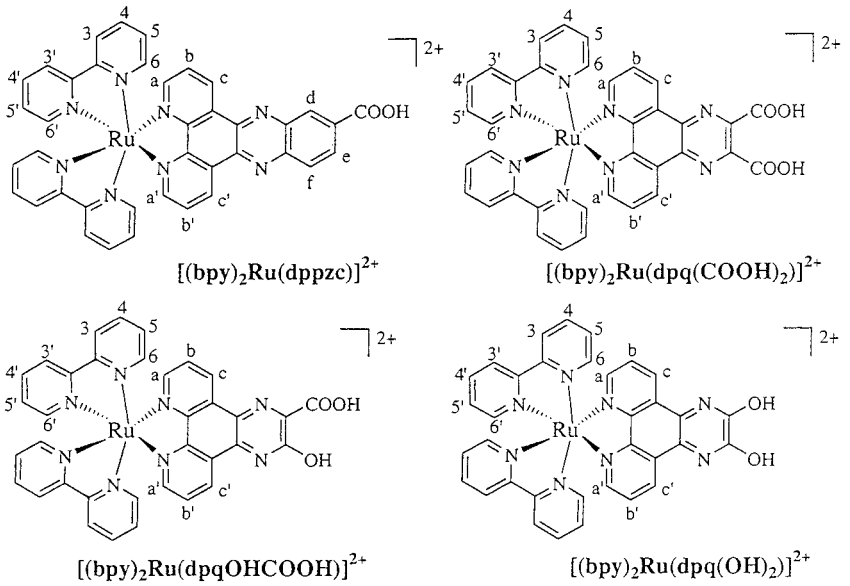

Figure 1. Structure and proton numbering of the Ru complexes synthesized in this work.

Furthermore, it has been well established that the introduction of carboxylic functional groups increases the adsorption of the metal complex on the TiO_2 surface. The interaction of this group with the surface Ti ions is likely to lead to the formation of hydrogen or ester bonds (C−O−Ti).[6] In the present study, we wish to report the use of hydroxyl functionals as the interlocking group for dye grafting to the TiO_2 surface.

In recent years, ligands derived from a modification of 2,2′-bipyridine (bpy) and 1,10-phenanthroline (phen) have been employed for certain applications.[5] We have synthesized a series of new complexes based on derivatives of the fully conjugated and planar ligands dipyrido[3,2-*a*:2′,3′-*c*]phenazine (dppz) and dipyrido[3,2-*f*:2′,3′-*h*]quinoxaline (dpq), two heteroaromatic entities obtained by fusing phenazine and quinoxaline subunits, respectively, to bpy. Among a great number of bridging ligands containing groups, these rigid π-conjugated systems are ideal selections because they prevent the bending along and/or rotation around the σ-skeleton of the molecule. In addition, π-electron conjugation over the aromatic parts allows a long-distance, yet sufficiently strong electronic interaction between those units.[5b]

From the viewpoint of structure, an ideal rigid system of photophysical interest would be a pair of electronically suitable D, in our system a Ru complex, and A, the nanocrystalline TiO_2 semiconductor, connected by a bridging ligand along one of the coordination axes yielding a linear structure.[5c] Using a number of hydroxyl- and/or carboxyl-substituted dpq, and dppz as the bridge, we report electrochemical and luminescence properties of their Ru complexes, and the results of an investigation on an electron-injection process (from (^3CT)Ru excited state to the conduction band of TiO_2) and corresponding incident-photon-to-current conversion efficiencies (IPCE). This is one of the few reports on utilization of hydroxyl binding for dye grafting to the nanocrystalline TiO_2 surfaces.[6c] The structures of the metal complexes synthesized in this study are illustrated in Figure 1.

Experimental Section

Instrumentation and Measurements. Absorption spectra were measured on a Hitachi 330 spectrophotometer. Emission spectra were recorded with a Hitachi F-3000 fluorescence spectrophotometer, which had been calibrated with a standard NBS tungsten−halogen lamp. Emission spectra were corrected for detector sensitivity using *N*,*N*-dimethyl-*m*-nitroaniline (10^{-4} M in benzene/hexane, 30:70) which was purified by recrystallization from acetone/benzene.[7] Emission lifetimes of the metal complexes, both in solution and anchored to nanocrystalline TiO_2, were measured with a Horiba NAES-1100 time-correlated single-photon counting system (excitation source was a nanosecond H_2 lamp, NFL-111, and the instrument response was less than 1 ns). The dye solutions were bubble degassed for 20 min with purified argon. For measuring emission lifetimes shorter than 1 ns in sensitized-TiO_2 electrodes, a time-correlated single-photon counting system with a cavity-dumped Ti^{3+}-sapphire laser was used (the instrument response is 40 ps).[8] This single-photon counting measurement and nano- and picosecond laser spectroscopy were performed in Photochemistry Lab, Osaka University, and the instrument details have been reported previously.[8b]

Electrospray ionization mass spectroscopy (ESI-MS) was performed with a Hitachi M1200H LC/MS system using methanol as eluant unless described otherwise.

Redox potentials of metal complexes were measured by cyclic and differential-pulse voltammetry using a BAS model 100B potentiostat in a standard three-cell electrode arrangement. Voltammograms were recorded using a platinum electrode (diameter 0.5 mm) in a solution of the complexes containing 0.1 M supporting electrolyte.

Materials. Acetonitrile (MeCN) was purified by fractional distillation from P_2O_5 after being maintained for 1 day over 4A molecular sieves.[9] In all cases where needed the distillation was repeated, and the center cut taken for use. All spectroscopic data were obtained on samples dissolved in the purified or spectral grade solvents. Hydrated ruthenium trichloride was purchased from Kojima Chemicals and used as received. All other reagents were reagent grade quality and used without further purification.

Synthesis. 1,10-Phenanthroline-5,6-dione (phenO_2),[10] [Ru(bpy)$_2$Cl$_2$]·2H$_2$O,[11] [(bpy)$_2$Ru(phenO_2)](PF$_6$)$_2$,[12] [Ru(DMSO)$_4$Cl$_2$], [(bpy)Ru(DMSO)$_2$-

(6) (a) Striplin, D. R.; Wall, C. G.; Erickson, B. W.; Meyer, T. J. *J. Phys. Chem. B* **1998**, *102*, 2383. (b) Nazeeruddin, M. K.; Kay, A.; Rodicio, I.; Humphry-Baker, R.; Muller, E.; Liska, P.; Vlachopoulos, N.; Grätzel, M. *J. Am. Chem. Soc.* **1993**, *115*, 6382. (c) Hou, Y.; Xe, P.; Zhang, B.; Cao, Y.; Xiao, X.; Wang, W. *Inorg. Chem.* **1999**, *38*, 6320.

(7) Melhuish, W. H. *Appl. Opt.* **1975**, *14*, 26.

(8) (a) Tsushima, M.; Ikeda, N.; Nozaki, K.; Ohno, T. *J. Phys. Chem. A* **2000**, *104*, 5176. (b) Gholamkhass, B.; Nozaki, K.; Ohno, T. *J. Phys. Chem. B* **1997**, *101*, 9010.

(9) Riddick, J. A.; Bunger, W. B.; Sakano, T. K. *Organic Solvents*, 4th ed.; Wiley: New York, 1986; Vol. 2, p 587.

Cl_2], and [(phen)Ru(DMSO)$_2$Cl$_2$][13] were prepared according to the literature methods.

One bridging-ligand containing compound [(bpy)$_2$Ru(dppzc)](PF$_6$)$_2$ was synthesized according to a similar method used for [(phen)$_2$Ru(dppzc)](PF$_6$)$_2$.[5h] For this compound and other dppzc- and dpq-containing compounds, the synthesis and purification methods used are described below. We note that similar sister compounds with bpy and phen have been reported in the literature.[5h,14]

(a) Dipyrido[3,2-*a*:2′,3′-*c*]phenazine-2-carboxylic Acid, dppzc. 3,4-Diaminobenzoic acid (30.4 mg) was added to a solution of 42 mg of phenO$_2$ in ethanol (20 mL). Within 5 min a creamy white precipitate was formed, and the mixture was allowed to reflux for 30 min, cooled down, and filtered. It was washed with several portions of ethanol. The crude was then dispersed in hot methanol and filtered, washed thoroughly with methanol, and dried under vacuum. Yield: 40 mg (61%). Anal. Calcd for $C_{19}H_{10}O_2N_4$: C, 69.94; H, 3.09; N, 17.17. Found: C, 69.41; H, 3.27; N, 17.05. ^{1}H NMR [DMSO-d_6] δ (ppm), multiplicity, integration, assignment: 9.66, ddd, 2H, a; 9.32, ddd, 2H, c; 8.98, s, 1H, d; 8.54, s, 2H, ef; 8.05, ddd, 2H, b.

(b) [(bpy)$_2$Ru(dppzc)](PF$_6$)$_2$. A solution of 30 mg of 3,4-diaminobenzoic acid in hot methanol (20 mL) was added to 120 mg of [bpy]$_2$Ru(phenO$_2$)](PF$_6$)$_2$·2H$_2$O dissolved in MeCN (10 mL) at near boiling point. The reaction mixture was refluxed for 1 h and subsequently cooled and concentrated. A saturated solution of NH_4PF_6 in water was added to precipitate the product. The orange-colored product was filtered and washed with water and ethanol. Purification by chromatography on SP Sephadex C-25 was performed with a mixture (1:1) of MeCN and aqueous buffer (pH = 5.0, containing 20 mM NH_4PF_6) as eluant. After elution of the unreacted starting materials, a center cut of the orange band was collected. Again saturated solution of NH_4PF_6 was added to the concentrate, and the precipitate was recrystallized from methanol/MeCN/saturated NH_4PF_6 to yield 106 mg (79%) of orange microcrystals. Anal. Calcd for $C_{39}H_{26}O_2N_8P_2F_{12}Ru$: C, 45.68; H, 2.50; N, 10.54. Found: C, 45.49; H, 2.55; N, 10.88. ^{1}H NMR [CD_3CN]: 7.25, ddd, 2H, 5′; 7.45, ddd, 2H, 5; 7.73, d, 2H, 6′; 7.84, d, 2H, 6; 7.88, ddd, 2H, bb′; 8.01, ddd, 2H, 4′; 8.10, ddd, 2H, 4; 8.16, dd, 2H, cc′; 8.44, dd, 1H, f; 8.52, dd, 4H, 33′; 8.68, dd, 1H, e; 9.02, s, 1H, d; 9.69, dd, 2H, aa′. ESI-MS: m/z = 370, [M − 2PF$_6$]$^{2+}$; 739, [M − 2PF$_6$ − H]$^+$; 885, [M − PF$_6$]$^+$.

(c) [(bpy)Ru(dppzc)$_2$](PF$_6$)$_2$. A mixture of [(bpy)Ru(DMSO)$_2$Cl$_2$] (30 mg, 0.062 mmol) and dppzc (40 mg, 0.123 mmol), in Ar-purged ethylene glycol (5 mL), was heated for 1 h at 130−140 °C. The solution was then cooled to room temperature, and an equal volume of saturated NH_4PF_6 in water was added. The red precipitate was filtered and washed thoroughly with water. The crude was dissolved in a mixture of MeCN/H_2O/H_2SO_4 (45:45:10) and refluxed overnight (hydrolysis of the ester bond formed by reaction of carboxylic moiety and ethylene glycol at high temperature). After 24 h, the reaction mixture was cooled down and to the concentrate was added an aqueous solution of NH_4PF_6. A red precipitate formed, which was filtered, washed with water, ethanol, and ether, and vacuum dried. Purification of this compound was performed by recrystallization from a mixture of MeCN, H_2O, and CF_3COOH. Yield: 42 mg (65%). Anal. Calcd for $C_{48}H_{28}O_4N_{10}P_2F_{12}Ru$: C, 48.05; H, 2.35; N, 11.67. Found: C, 48.07; H, 2.58; N, 11.59. ^{1}H NMR [CF_3COOD]: 7.53, dd, 2H, 5; 7.97, dd, 2H, b′; 8.09, dd, 2H, 6; 8.17, dd, 2H, b; 8.25, dd, 2H, 4; 8.42, dd, 2H, c′; 8.52, dd, 2H, c; 8.73, d, 2H, ff′; 8.78, dd, 2H, 3; 8.88, dd, 2H, ee′; 9.49, s, 1H, d′; 9.52, s, 1H, d; 9.96, d, 2H, a′, 10.05, d, 2H, a. ESI-MS: m/z = 455, [M − 2PF$_6$]$^{2+}$; 606, [M$_2$ − 4PF$_6$ − H$^+$]$^{3+}$; 909, [M − 2PF$_6$ − H]$^+$; 1055, [M − PF$_6$]$^+$.

(d) [(phen)Ru(dppzc)(dppzCOO)](PF$_6$)·4H$_2$O. A mixture of [(phen)Ru(DMSO)$_2$Cl$_2$] (118 mg, 0.232 mmol) and dppzc (152 mg, 0.466 mmol), in Ar-purged ethylene glycol (10 mL), was heated for 3 h at 135−140 °C. The following steps were the same as those mentioned for [(bpy)Ru(dppzc)$_2$](PF$_6$)$_2$. Yield: 118 mg (47%). Anal. Calcd for $C_{50}H_{27}O_4N_{10}PF_6Ru$·4H$_2$O (singly deprotonated): C, 52.23; H, 3.07; N, 12.18. Found: C, 52.74; H, 2.63; N, 11.70. ^{1}H NMR [CF_3COOD]: 7.68, dd, 2H, 3 (8); 7.83, overlapped, 4H, bb′b″; 8.16, dd, 1H, c″; 8.20, s, 2H, 5 (6); 8.24, d, 2H, 2 (9); 8.38, dd, 3H, cc′; 8.56, d, 2H, 4 (7); 8.59, d, 2H, f; 8.70, d, 2H, e; 9.33, s, 2H, d; 9.82, td, 4H, aa′a″. ESI-MS: m/z = 467, [M − 2PF$_6$]$^{2+}$; 622, [M$_2$ − 4PF$_6$ − H]$^{3+}$; 934, [M − 2PF$_6$ − H]$^+$.

(e) 2,3-Dicyanodipyrido[3,2-*f*:2′,3′-*h*]quinoxaline, dpq(CN)$_2$. Diaminomaleonitrile (162 mg, 1.5 mmol) and phenO$_2$ (210 mg, 1 mmol) were reacted in ethanol (50 mL) under reflux conditions. After 1 h, the reaction mixture was cooled to room temperature, concentrated, and kept in an ice bath. Pink-brown needles were formed, which were filtered, washed with ethanol, and dried. Yield: 229 mg (81%). The crude can be recrystallized from ethanol. Anal. Calcd for $C_{16}H_6N_6$: C, 68.08; H, 2.14; N, 29.77. Found: C, 67.70; H, 2.14; N, 29.80. ^{1}H NMR [$CDCl_3$]: 9.48, d, 2H, a; 9.42, d, 2H, c; 7.92, dd, 2H, b.

(f) [(bpy)$_2$Ru(dpq(CN)$_2$)](PF$_6$)$_2$·2H$_2$O. A solution of 46 mg of diaminomaleonitrile in hot methanol (5 mL) was added to 200 mg of [bpy]$_2$Ru(phenO$_2$)](PF$_6$)$_2$·2H$_2$O dissolved in hot MeCN (15 mL), and the reaction mixture was refluxed for 50 min. After cooling down to room temperature, the solution was concentrated with a rotary evaporator followed by addition of aqueous NH_4PF_6 saturated solution. The red precipitate was filtered and washed with cold water and ethanol. The product was subjected to a column chromatography on SP Sephadex C-25 using a 1:1 mixture of MeCN and aqueous buffer (pH = 4.1, containing 10 mM NH_4PF_6) as eluant. A center cut of the red band was collected. Again saturated solution of NH_4PF_6 in H_2O was added to the concentrate, and the precipitate was recrystallized by slow evaporation of acetone from methanol and water containing a minimum amount of NH_4PF_6 to yield 196 mg (88%) of red microcrystals. Anal. Calcd for $C_{36}H_{22}N_{10}P_2F_{12}Ru$·2H$_2$O: C, 42.32; H, 2.57; N, 13.71. Found: C, 42.50; H, 2.42; N, 13.56. ^{1}H NMR [CD_3CN]: 7.21, ddd, 2H, 5′; 7.43, ddd, 2H, 5; 7.51, dd, 2H, 6′; 7.77, dd, 2H, bb′; 7.80, dd, 2H, 6; 7.98, td, 2H, 4′; 8.05, dd, 2H, cc′; 8.09, td, 2H, 4; 8.50, dd, 4H, 3 (3′); 8.81, d, 2H, aa′. ESI-MS: m/z = 348, [M − 2PF$_6$]$^{2+}$; 841, [M −PF$_6$]$^+$.

(g) [(bpy)$_2$Ru(dpqOHCOOH)](PF$_6$)$_2$·H$_2$O. A portion of 40 mg of [(bpy)$_2$Ru(dpq(CN)$_2$)](PF$_6$)$_2$·2H$_2$O was dissolved in ethanol/MeCN (20:1). To this was added 4 mL of 0.2 M NaOH, and the mixture was deoxygenated before refluxing for a period of 2 h. At this stage, electrospray mass spectrometric measurement showed the production of [(bpy)$_2$Ru(dpqOHCOONa)]$^{2+}$ (m/z = 364). Thus treatment of [(bpy)$_2$Ru(dpq(CN)$_2$)]$^{2+}$ with OH$^-$ in ethanol results in substitution of one of the cyano groups by OH$^-$ (also see Mass Spectroscopy section) and at the same time hydrolysis of the other CN to COO$^-$. Nucleophilic substitution of a single CN in 1,2-dicyano organic compounds has been described in the literature.[15] Then the reaction mixture was cooled and concentrated. To the concentrate was added 2 mL of 1 N H_2SO_4 followed by 10 mL of H_2O (to dissolve initially formed Na_2SO_4). It was then heated at 80 °C for 1 h. After the mixture was cooled to 0 °C in an ice bath, a saturated aqueous solution of NH_4PF_6 was added to precipitate the complex. The orange precipitate formed was filtered, washed with cold water and ether, and vacuum-dried (crude yield: 30.3 mg, 75%). Purification can be performed by column chromatography on SP Sephadex C-25 followed by recrystallization from an EtOH/water mixture. Yield: 19 mg (47%). Anal. Calcd for $C_{35}H_{24}O_3N_8P_2F_{12}Ru$·H$_2$O: C, 41.47; H, 2.59; N, 11.05. Found: C, 41.94; H, 2.66; N, 10.64. ^{1}H NMR [CD_3CN]: 7.21, ddd, 2H, 5′; 7.43, ddd, 2H, 5; 7.55, dd, 2H, 6′; 7.78, dd, 2H, 6; 7.81, overlapped, 2H, 4′; 8.00, td, 2H, 4; 8.02, dd, 1H, b′; 8.07, dd, 1H, b; 8.10, dd, 2H, cc′; 8.50, dd, 4H, 3 (3′); 8.94, dd, 1H, a′; 9.21, dd, 1H, a. ESI-MS: m/z = 353, [M − 2PF$_6$]$^{2+}$; 705, [M − 2PF$_6$ − H]$^+$; 851, [M − PF$_6$]$^+$.

(h) [(bpy)$_2$Ru(dpq(COOH)$_2$)](PF$_6$)$_2$·0.5NH$_4$PF$_6$. [(bpy)$_2$Ru(dpq(CN)$_2$)](PF$_6$)$_2$·4H$_2$O (50 mg) was dissolved in 20 mL of warm 5M H_2SO_4, and the solution was deoxygenated before heating at 110−120 °C overnight. After cooling in an ice bath, the pH of this solution was increased to 4 by the addition of 5 M NaOH. An orange precipitate

(10) Amouyal, E.; Homsi, A.; Chambron, J.-C.; Sauvage, J.-P. *J. Chem. Soc., Dalton Trans.* **1990**, 1841.
(11) Sullivan, B. P.; Meyer, T. J. *Inorg. Chem.* **1978**, *17*, 3334.
(12) Goss, C. A.; Abruna, H. D. *Inorg. Chem.* **1985**, *24*, 4263.
(13) Evans, I. P.; Spencer, A.; Wilkinson, G. *J. Chem. Soc., Dalton Trans.* **1973**, 204.
(14) Arounaguiri, S.; Maiya, B. G. *Inorg. Chem.* **1999**, *38*, 842.
(15) Begland, R. W.; Hartter, D. R. *J. Org. Chem.* **1972**, *37*, 4136.

was formed upon addition of aqueous NH_4PF_6 and was filtered off and washed with a minimum amount of cold water. The same chromatographic purification was carried out again using a 1:1 mixture of MeCN and aqueous buffer (pH = 4.1, containing 20 mM NH_4PF_6) as an eluant. The main orange band was collected and precipitated by cooling the concentrate in an ice bath. The precipitate was filtered off, washed with cold water, and recrystallized from water containing NH_4PF_6. Yield: 44 mg (85%). Anal. Calcd for $C_{36}H_{24}O_4N_8P_2F_{12}Ru\cdot 0.5NH_4PF_6$: C, 39.13; H, 2.37; N, 10.77. Found: C, 39.15; H, 2.39; N, 10.94. ^{1}H NMR [CD_3CN]: 7.23, ddd, 2H, 5′; 7.44, ddd, 2H, 5; 7.66, dd, 2H, 6′; 7.83, dd, 2H, 6; 7.88, dd, 2H, bb′; 7.99, td, 2H, 4′; 8.09, td, 2H, 4; 8.18, dd, 2H, cc′; 8.50, dd, 4H, 3 (3′); 9.58, dd, 2H, aa′. ESI-MS: m/z = 367, $[M - 2PF_6]^{2+}$; 733, $[M - 2PF_6 - H]^+$; 879, $[M - PF_6]^+$.

(i) $[(bpy)_2Ru(dpq(OH)_2)](PF_6)_2\cdot 2H_2O$. $[(bpy)_2Ru(dpq(CN)_2)](PF6)_2\cdot 4H_2O$ (80 mg) was dissolved in 5 M NaOH (25 mL), and the mixture was refluxed overnight. Then the reaction mixture was cooled, and the pH of this solution was decreased to 6 by the addition of 1 N H_2SO_4. The product was precipitated by the addition of an aqueous solution of NH_4PF_6. The precipitate was filtered off and washed with cold water. The crude was purified chromatographically on SP Sephadex C-25. The eluant was a 1:1 mixture of MeCN and aqueous buffer (pH = 2.5, containing 50 mM NH_4PF_6). A center cut of the third red band was collected, reprecipitated, and recrystallized by slow evaporation of acetone from an acetone/water mixture. Yield: 20 mg (25%). Anal. Calcd for $C_{34}H_{24}O_2N_8P_2F_{12}Ru\cdot 2H_2O$: C, 40.69; H, 2.81; N, 11.16. Found: C, 40.75; H, 2.77; N, 10.55. ^{1}H NMR [CD_3CN]: 7.21, ddd, 2H, 5′; 7.43, ddd, 2H, 5; 7.51, dd, 2H, 6′; 7.77, dd, 2H, bb′; 7.80, dd, 2H, 6; 7.98, td, 2H, 4′; 8.04, dd, 2H, cc′; 8.08, td, 2H, 4; 8.50, dd, 4H, 3 (3′); 8.84, d, 2H, aa′. ESI-MS: m/z = 339, $[M - 2PF_6]^{2+}$; 823, $[M - PF_6]^+$.

All the Ru complexes were obtained as PF_6^- salts, and in the case where necessary they could be quantitatively converted to chloride salts by reacting with tetra-*n*-butylammonium chloride in acetone. These chloride salts were soluble in water and alcoholic solvents.

Preparation of TiO_2 Films. Thin TiO_2 films were prepared by thermal decomposition of titanium alkoxide deposited on glass plates. Those plates were dip-coated in a mixture of tetrapropyl orthotitanate, ethanol, poly(ethylene glycol) with an average molecular weight of 300−1000, and 2-(2-ethoxyethoxy)ethanol under a relative humidity of 10%. The dip-coated glass plates were calcified at 450 °C for 1 h. The XRD profiles of the TiO_2 thin films showed that an anatase crystalline structure was formed without any contamination of the other phase of TiO_2. The procedure details were reported previously.[16]

Dye Coating of the TiO_2 Electrodes. All the Ru complexes were coated onto the TiO_2 films by dipping the glass plates for ca. 12 h in a 10^{-5}−10^{-4} M solution of the compound in MeCN. The TiO_2 films assumed a yellow color due to adsorption of the dye. After rinsing of the plates several times with acetone, no leaching of the dye into solution could be detected using luminescence spectroscopy. Photoelectrochemical experiments were performed on these sensitized plates using them as the working electrode in a three-compartment cell. The TiO_2 electrode was mounted on a homemade cell compartment containing ~3 mL of MeCN solution 0.1 M in tetraethylammomium iodide and 0.05 M in I_2. To avoid absorption of light by a rather concentrated solution of I_2/I^-, the incident beam was allowed to pass first through the rear side of the TiO_2 electrode, with its front side facing the electrolyte, and then into the solution. The excitation beam was collected from the light source of a Hitachi (F-3000) fluorescence spectrophotometer, and redirected toward either a LEO/CDI optical spectrograph for light intensity measurement or the sensitized-TiO_2 electrode mounted on the photochemical cell compartment. The counter electrode was a Pt wire. The incident-photon-to-current conversion efficiencies (IPCE) at each wavelength were calculated from the ratio of the photocurrent (μA/cm^2) to the photon flux (μW/cm^2). No effort was made to maximize the IPCE values.

Results and Discussion

Absorption and Emission Spectra. The absorption spectra of selected metal complexes are shown in Figure 2 while Table 1 lists absorption and emission maxima, molar extinction coefficients, emission lifetimes, and quantum yields for all the complexes. For the metal complexes, absorption features appearing in the UV region (λ < 350 nm) can be ascribed to spin-allowed, ligand-centered transitions with the intense band at ca. 286 nm being associated with polypyridine units presented in the structure. Absorption bands in the visible region (350−600 nm) correspond to spin-allowed ^{1}MLCT transitions.

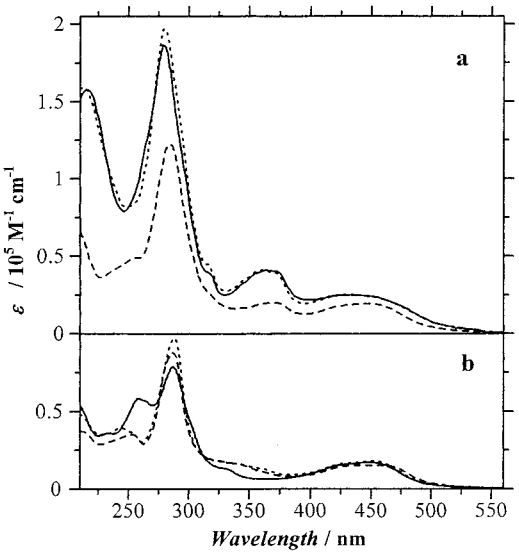

Figure 2. Absorption spectra and molar extinction coefficient of (a) $[(bpy)_2Ru(dppzc)]^{2+}$ (dashed line), $[(bpy)Ru(dppzc)_2]^{2+}$ (10^{-2} M TFAc, dotted line), and $[(phen)Ru(dppzc)_2]^{2+}$ (10^{-2} M TFAc, solid line), and (b) $[(bpy)_2Ru(dpq(OH)_2)]^{2+}$ (dashed line), $[(bpy)_2Ru(dpqOHCOOH)]^{2+}$ (dotted line), and $[(bpy)_2Ru(dpq(COOH)_2)]^{2+}$ (solid line), in MeCN at room temperature.

As seen for dppzc-containing complexes (Figure 2a), the spectra retain most of the features of the components, $[Ru(bpy)_2]$ and the bridging ligand moiety, dppz.[17] They display a strong MLCT band at around 450 nm attributed to the $d\pi(M) \rightarrow \pi^*$-(dppzc and bpy or phen), without any appreciable resolution of transitions involving different ligands. At shorter wavelengths (360−380 nm), two bands appear in the spectra which are not as sharp as those of the dppz moiety itself.[16] These probably correspond to intraligand ($\pi \rightarrow \pi^*$) transitions in the dppzc, while at ca. 285 nm and below that the strong bands can be attributed to the overlap of bpy (or phen) and dppzc $\pi \rightarrow \pi^*$ transitions.

In the case of bis-dppzc complexes, $[(bpy)Ru(dppzc)_2](PF_6)_2$ and $[(phen)Ru(dppzc)_2](PF_6)_2$, the most important point to note is an exact two times increase in the molar extinction coefficient in the 360−380 nm region compared with that of the mono-dppzc (Figure 2a). The molar absorptivities in this spectral region (Table 1) scale as the total number of electronically decoupled dppzc ligands presented in the complex.

For the $dpq(CN)_2$ ligand, those peaks appeared at 365 and 344 nm, the latter as a shoulder of the main peak centered at 304 nm. In its Ru complex, $[(bpy)_2Ru(dpq(CN)_2)]^{2+}$, these are blue shifted to 348 and 333 nm (shoulder), due to coordination to the metal center. In the other related compounds, $[(bpy)_2Ru(dpq(COOH)_2)]^{2+}$, $[(bpy)_2Ru(dpqOHCOOH)]^{2+}$, and $[(bpy)_2Ru(dpq(OH)_2)]^{2+}$, only a broad band was observed in this region (Figure 2b).

(16) Negishi, N.; Takeuchi, K.; Ibusuki, T. *J. Mater. Sci.* **1998**, *33*, 5789.

(17) Yamada, M.; Tanaka, Y.; Yoshimoto, Y.; Kuroda, S.; Shimao, I. *Bull. Chem. Soc. Jpn.* **1992**, *65*, 1006.

Table 1. Spectroscopic and Photophysical Properties for the Ru Complexes[a]

compound	λ_{abs}[b]/nm (ϵ_{max}[c]/10^3 M^{-1} cm^{-1})		λ_{em}[b]/nm		τ[d]/ns	ϕ_{em}[e]
	$\pi-\pi^*$	MLCT	298 K	77 K	298 K	298 K
$[(bpy)_2Ru(dppzc)]^{2+}$	255[f] (49.1), 285 (123.0), 364 (19.9), 372 (19.9)	448 (19.5)	630	602	1000	0.009
$[(bpy)Ru(dppzc)_2]^{2+}$ [g]	280 (196.9), 315[f] (44.5), 362 (40.8), 371 (39.1)	431 (25.1)		593	760[h]	
$[(phen)Ru(dppzc)_2]^{2+}$ [g]	286 (186.7), 315[f] (40.0), 363 (40.7), 372 (40.3)	431 (24.3)		591		
$[(bpy)_2Ru(dpq(CN)_2)]^{4+}$	264 (80.3), 286 (84.3), 348 (11.2)	439 (17.5)	640	580	77[i]	0.0055
$[(bpy)_2Ru(dpq(COOH)_2)]^{2+}$	258 (58.5), 287 (79.0)	449 (17.2)	622	590	910	0.062
$[(bpy)_2Ru(dpqOHCOOH)]^{2+}$	244 (39.2), 287 (96.7)	455 (17.8)	620	581	1250	0.068
$[(bpy)_2Ru(dpq(OH)_2)]^{2+}$	252 (35.0), 286 (87.8)	453 (15.6)	627	589	2150	0.087

[a] All the complexes are PF_6 salts, and the values are obtained in MeCN at room temperature unless otherwise mentioned. [b] Uncertainty in λ_{abs} and λ_{em} is ± 1 nm. The emission maximum at 77 K is taken in *n*-butyronitrile glass. [c] Estimated error in ϵ_{max} is $\pm 5\%$. [d] Uncertainty in lifetime values is <6%. For comparison, the emission decay rate for $[Ru(bpy)_3]^{2+}$ was also measured; under identical conditions it has a lifetime of 850 ns. [e] Emission quantum yields relative to $[Ru(bpy)_3]^{2+}$: $\phi_{em} = 0.061$. [f] Appeared as a shoulder. [g] In MeCN containing 10^{-2} M triflouroacetic acid. [h] In Ar-purged DMF. [i] Time-resolved transient absorption spectroscopy at 450 nm gives a value of 96 ns for the excited-state lifetime of this complex.

Table 2. Redox Potentials (mV) of Ru Complexes[a]

compound	$E_{1/2}$(ox)	$E_{1/2}$(red)
$[Ru(bpy)_3]^{2+}$	+880	−1690, −1890, −2140
$[Ru(bpy)_3]^{2+}$ [b]	+820	−1690, −1870, −2140
$[(bpy)_2Ru(dppzc)]^{2+}$	+910	
$[(bpy)_2Ru(dppzc)]^{2+}$ [b]	+850	−1400, −1810, −1980, −2230
$[(bpy)Ru(dppzc)_2]^{2+}$	+885	−1170, −1280, −1870, −2030, −2220
$[(phen)Ru(dppzc)_2]^{2+}$	+905	−1150, −1280, −1870, −2080, −2270
$[(bpy)_2Ru(dpq(CN)_2)]^{2+}$	+980	−940, −1360, −1800, −2040, −2210
$[(bpy)_2Ru(dpq(CN)_2)]^{2+}$ [b]	+940	−1000, −1300, −1830, −2080, −2380
$[(bpy)_2Ru(dpq(COOH)_2)]^{2+}$	+940	−1270, −1750, −2010, −2250
$[(bpy)_2Ru(dpq(COOH)_2)]^{2+}$ [b]	+880	−1415, −1780, −1955, −2225
$[(bpy)_2Ru(dpqOHCOOH)]^{2+}$	+910	−1770, −2000, −2300
$[(bpy)_2Ru(dpqOHCOOH)]^{2+}$ [b]		−1800, −2010, −2370, −2900
$[(bpy)_2Ru(dpq(OH)_2)]^{2+}$	+940	−1810, −1990, −2270, −2370
$[(bpy)_2Ru(dpq(OH)_2)]^{2+}$ [b]		−1790, −1980, −2180, −2380, −2880

[a] At room temperature and in MeCN solutions containing 0.1 M tetra-*n*-butylammonium hexafluorophosphate (TBAH). All $E_{1/2}$ values are referred to $E_{1/2}$ of the ferrocenium$^+$/ferrocene redox couple (380 mV vs SCE in MeCN), and for comparison the redox potentials of $[Ru(bpy)_3]^{2+}$ are also presented. [b] In DMF (0.1 M TBAH).

Emission band maxima and lifetimes for all of the Ru complexes are presented in Table 1. A single emission was observed for all of the complexes. They exhibit the characteristic MLCT luminescence both in fluid solution at room temperature and in glass matrix at 77 K.[4a,18] This assignment is based on the following luminescence properties: (i) at room temperature the emission spectra of the metal complexes are broad and structureless and the lifetimes, with the exception of $[(bpy)_2Ru(dpq(CN)_2)]^{2+}$, are similar to that of $[Ru(bpy)_3]^{2+}$ whose emission was previously assigned as coming from ^{3}MLCT states;[4a,19] (ii) at 77 K the emission spectra show vibrational progression with spacing of ca. 1300 cm^{-1}, as expected for Ru−polypyridine emitters in frozen solvent, and are centered at a slightly shorter wavelength than at room temperature.[20]

In the case of $[(bpy)_2Ru(dpq(CN)_2)]^{2+}$, the luminescence lifetime (τ < 100 ns) is extraordinarily shorter than those of ruthenium polypyridine complexes (typically in the microsecond range). Additionally, its sister compound, $[(phen)_2Ru(dpq(CN)_2)]^{2+}$, exhibited a "molecular light switch" effect.[14] In the presence of DNA, this compound shows an increase in the emission intensity which is less pronounced compared to $[(phen)_2Ru(dppz)]^{2+}$.[21] The light switch mechanism in these complexes has been attributed to an excited-state interconversion of the initially formed $MLCT_1$ to a different emitting $MLCT_2$, which itself has a rapid nonradiative decay pathway.[21] From the data in Table 1, radiative and nonradiative decay rates, k_r and k_{nr}, can be calculated using the equation $k_r = \phi_{em}/\tau$ where $\tau = 1/(k_r + k_{nr})$ and ϕ_{em} is the quantum yield of emission. For $[(bpy)_2Ru(dpq(CN)_2)]^{2+}$ and $[(bpy)_2Ru(dpq(OH)_2)]^{2+}$, the obtained k_{nr} values are 1.3×10^7 and 4.2×10^5 s^{-1}, respectively. Therefore, short excited-state lifetime and low quantum yield of emission in $[(bpy)_2Ru(dpq(CN)_2)]^{2+}$ are largely consequences of this rapid nonradiative decay. On the other hand, longer lifetime of the excited state in $[(bpy)_2Ru(dpq(OH)_2)]^{2+}$ can also be correlated to its slow nonradiative decay. Small k_{nr} in this complex may originate from the stronger σ-donor ability of the ligand $dpq(OH)_2$ and subsequent destabilization of the $d\sigma^*$ orbital giving a wider $d\pi-d\sigma^*$ energy gap.[22]

Electrochemistry. The electrochemical properties of dpq complexes have been studied in MeCN. As for mono- and bis-dppzc complexes, in addition to the poor solubility of the bis compounds, the reductions are not well behaved in MeCN, probably due to adsorption of the reduced species onto the electrode surface. For this series of complexes, the redox processes have been studied in DMF using a carbon disk as a working electrode. The number of electrons involved in each process has been estimated by pulsed differential voltammetry. The half-wave potentials are presented in Table 2. For com-

(18) Kober, E. M.; Caspar, J. V.; Sullivan, B. P.; Meyer, T. J. *Inorg. Chem.* **1988**, *27*, 4587.
(19) (a) Meyer, T. J. *Pure Appl. Chem.* **1986**, *58*, 1193. (b) Kalyanasundaram, K. *Coord. Chem. Rev.* **1982**, *46*, 159.
(20) (a) Caspar, J. V.; Meyer, T. J. *Inorg. Chem.* **1983**, *22*, 2444. (b) Kober, E. M.; Caspar, J. V.; Lumpkin, R. S.; Meyer, T. J. *J. Phys. Chem.* **1986**, *90*, 3722. (c) Barkawi, K. R.; Murtaza, Z.; Meyer, T. J. *J. Phys. Chem.* **1991**, *95*, 97.
(21) Olson, E. J. C.; Hu, D.; Hörmann, A.; Jonkman, A. M.; Arkin, M. R.; Stemp, E. D. A.; Barton, J. K.; Barbara, P. F. *J. Am. Chem. Soc.* **1997**, *119*, 11458.
(22) Kalyanasundaram, K. *Photochemistry of Polypyridine and Porphyrin Complexes*; Academic Press Inc.: San Diego, 1992.

parison purposes, the redox potentials of $[Ru(bpy)_3]^{2+}$ are also included.

Cyclic voltammograms of the complexes are consistent with a metal-based reversible oxidation and several ligand-based reductions. By analogy with similar complexes such as $[Ru(bpy)_3]^{2+}$ and $[Ru(bpy)_2phen]^{2+}$, for most of the complexes, we assign the first reduction wave to the dppzc and dpq ones. These reduction potentials are anodically shifted with respect to that of $[Ru(bpy)_3]^{2+}$, which emphasizes the enhanced π-electron acceptor characteristics of dppzc and dpq. However, for $[(bpy)_2Ru(dpqOHCOOH)]^{2+}$ and $[(bpy)_2Ru(dpq(OH)_2)]^{2+}$, the first reduction wave is close to the one in $[Ru(bpy)_3]^{2+}$, making it rather difficult to ascribe this potential. In bis-dppzc compounds, the first and second reductions at about -1160 and -1280 mV can be attributed to the reductions of two dppzc ligands, which are then followed by reduction of bpy or phen. Also in $[(bpy)_2Ru(dppzc)]^{2+}$ and $[(bpy)_2Ru(dpq(COOH)_2)]^{2+}$, the second and third reduction potentials as well as their differences are comparable to the first and second reductions and their corresponding differences in $[Ru(bpy)_3]^{2+}$. This could be an indication of the lack of any important orbital overlap between the unoccupied bpy-like molecular orbitals (MOs that are involved in the reduction process) and the lowest MO developed, most likely, on the phenazine or quinoxaline heteroaromatic part of the dppzc and $dpq(COOH)_2$.

In this series of compounds, the oxidation wave occurs at potentials slightly more positive than the $Ru^{3+/2+}$ couple in $[Ru(bpy)_3]^{2+}$, the smallest shift being in $[(bpy)_2Ru(dppzc)]^{2+}$ (30 mV) and the largest in $[(bpy)_2Ru(dpq(CN)_2)]^{2+}$ and $[(bpy)_2Ru(dpq(COOH)_2)]^{2+}$ (80 mV). This trend is commonly observed in complexes containing π-acceptor ligands.[22] However, the increased difference on going from dppzc to dpq is consistent with an increasing contribution from the heteroaromatic part to the HOMO which has a MO character very similar to that of $[Ru(bpy)_3]^{2+}$. Furthermore, when considering a simple electronic approach, this may be a result of pronounced π-acceptor character due to a shorter distance between the HOMO, which is localized (or rather centered) on the metal,[5b,23] and the π-withdrawing groups ($-$CN or $-$COOH) in dpq compared to dppzc. Indeed, we found more evidence in supporting the present argument resulting from pK_a measurement (vide infra).

Mass Spectroscopy. All of the complexes were further characterized by electrospray mass spectroscopy (ES-MS) in either a MeOH, MeCN, or MeCN/CF_3COOH mixture. Peaks of perfectly resolved state of charge, i.e., $[M - PF_6]^+$ and $[M - 2PF_6]^{2+}$ were observed at corresponding *m*/*z*.

For $[(bpy)_2Ru(dppzc)]^{2+}$, a main peak was also detected at *m*/*z* 739 which corresponds to the deprotonated form $[M - 2PF_6 - H]^+$. Due to the poor solubility of bis-dppzc complexes, these samples were dissolved in MeCN containing a small amount of CF_3COOH and subjected to ESI-MS measurement. In these complexes, while the $[M - PF_6]^+$ peak was hardly observed, the deprotonated dimer structure $[M_2 - 4PF_6 - H]^{3+}$ and the deprotonated monomer $[M - 2PF_6 - H]^+$ were detected at *m*/*z* 606.4 and 622.4 for $[(bpy)Ru(dppzc)_2]^{2+}$ and $[(phen)Ru(dppzc)_2]^{2+}$, respectively. From this observation, it appears that bis-dppzc complexes are prone to form deprotonated and dimerized structures even in acidic solutions. Note that, in the case of $[(phen)Ru(dppzc)_2]^{2+}$, the CHN analytical result matches a deprotonated mono anionic salt, i.e., $[(phen)Ru^{II}(dppzCOOH)(dppzCOO^-)]PF_6 \cdot 4H_2O$. Thus poor solubility can be explained in terms of aggregation behavior as a direct result of well-counterbalanced intermolecular Coulombic repulsions against van der Waals and/or ionic interactions following deprotonation. Aggregation in solution of ruthenium complexes bearing large heteroaromatic ligands has previously been described in the literature.[5d,24]

As for $[(bpy)_2Ru(dpq(CN)_2)]^{2+}$, when the ESI-MS measurement was performed in MeOH, a net chemical reaction occurred and one of the $-$CN groups was substituted by $-OCH_3$ (coming from the solvent) leading to observation of the peaks at *m*/*z* 350.6 and 846.0. Using the same load of sample, the measurement was also carried out in MeCN and peaks were detected at *m*/*z* 348 and 841 corresponding to $[M - 2PF_6]^{2+}$ and $[M - PF_6]^+$, respectively.

Proton NMR. All complexes were characterized by ^1H and where needed $^1H-^1H$ COSY NMR spectroscopy. For most of the complexes, the proton NMR signals were unambiguously assigned (see Experimental Section). It must be pointed out that the bpy protons H_5 and $H_{5'}$, which should be normally observed with multiplicity defined as "doublet of doublets" (dd), were degenerated to two sets of dd due to the fact that they may experience different environments regarding the spatial conformation of the molecule. An overlap of those two sets gives rise to a new multiplicity defined here as doublet of "doublet of doublets" (ddd).

As observed for mono- and bis-dppzc complexes comprising a large aromatic part, the chemical shifts were less sensitive (<0.05 ppm) to concentration compared with tetrapyrido[3,2-*a*:2′,3′-*c*:3″,2″-*h*:2‴,3‴-*j*]phenazine (tpphz) complexes for which a strong dependence on concentration has been observed.[5b−d] Nevertheless, the most affected protons are the dppzc protons, which move downfield along with increased concentration due to $\pi-\pi$ stacking of the heteroaromatic part. This property, however, is less pronounced when compared to tpphz complexes probably because of the smaller aromatic conjugated system. In the dpq complexes, for the same reason, the resonance signals are not concentration dependent.

The ^1H NMR spectrum of $[(bpy)_2Ru(dppzc)]^{2+}$ was also measured in CF_3COOD. It is interesting to notice that while all of the resonance signals are downfield shifted with an average $\Delta\delta$ of 0.15 ppm, the phenazine protons H_d and H_f are the most affected ones ($\Delta\delta = 0.46$ and 0.3 ppm, respectively). It seems that the phenazine nitrogens (located very close to H_d and H_f positions) are more solvent-accessible, and in fact they are the most likely sites of solvent association via hydrogen bonds. In this respect, we have also examined the effect of water on $[(bpy)_2Ru(dppzc)]^{2+}$ excited-state quenching in predominantly nonaqueous solvents.

Quenching of $[(bpy)_2Ru(dppzc)]^{2+}$ Excited State by Water. The mono-dppzc complex, like its two related sister compounds, $[(bpy)_2Ru(dppz)]^{2+}$ and $[(phen)_2Ru(dppz)]^{2+}$,[10,23a,25] shows no photoluminescence in aqueous solution but emits in nonaqueous solvents such as MeOH, MeCN, or DMF. In general, Stern−Volmer (SV) plots of emission intensity in these solvents when quenched by water (0−7 M in concentration) are not linear. The Perrin sphere (PS) of the quenching model was found to fit the data much better than the SV model. In the PS model, eq 1, the quencher molecules are able to quench the excited

(23) (a) Chambron, J.-C.; Sauvage, J.-P.; Amouyal, E.; Koffi, P. *Nouv. J. Chim.* **1985**, *9*, 527. (b) Fees, J.; Kaim, W.; Moscherosch, M.; Matheis, W.; Klima, J.; Krijcicik, M.; Zalis, S. *Inorg. Chem.* **1993**, *32*, 166. (c) Ishow, E.; Gourdon, A.; Launay, J.-P.; Lacante, P.; Verelst, M.; Chiorboli, C.; Scandola, F.; Bignozzi, C.-A. *Inorg. Chem.* **1998**, *37*, 3603. (d) Ishow, E.; Gourdon, A.; Launay, J.-P.; Chiorboli, C.; Scandola, F. *Inorg. Chem.* **1999**, *38*, 1504.

(24) Ruminski, R. R.; Kiplinger, J. L. *Inorg. Chem.* **1990**, *29*, 4581.

(25) Nair, R. B.; Cullum, B. M.; Murphy, C. J. *Inorg. Chem.* **1997**, *36*, 962.

Table 3. Fitting Parameters for Perrin Sphere Quenching of $[(bpy)_2Ru(dppzc)]^{2+}$ by H_2O (0−8 M), in Nonaqueous Solvents[a]

solvent	[Ru]/M	slope	*r*(Å)	correlation coeff
MeCN	2×10^{-5}	0.61 ± 0.03	6.2	0.997
MeOH	1×10^{-5}	0.31 ± 0.006	5.0	0.998
DMF	1×10^{-5}	0.51 ± 0.08	5.9	0.999

[a] At room temperature and in air-saturated solutions containing a $1-2 \times 10^{-5}$ M concentration of the title complex.

molecules only if they are within a sphere of radius *r*,[26]

$$\mathrm{Ln}\,(\phi_0/\phi) = N_A V\,[\mathrm{Q}] \qquad (1)$$

In this equation, ϕ and ϕ_0 are the relative quantum yields of emission with and without quencher, respectively, N_A is Avogadro's number, V ($(4/3)\pi r^3$) is the volume of the quenching sphere, and [Q] is the quencher (in this case H_2O) concentration. Values for *r* and fit parameters are gathered in Table 3. From this table it appears that the radius of water quenching (5.0−6.2 Å) depends on the applied solvent; the better the solvent molecule is at hydrogen bonding, the smaller the radius ($r_{MeOH} < r_{DMF} < r_{MeCN}$). Together with NMR data in CF_3COOD, this experimental evidence indicates the importance of the microenvironment around the phenazine nitrogens, and the fact that static quenching may contribute to the quenching process.

Measurement of pK_a. The pK_a's of the Ru complexes were determined by means of spectrophotometric titration. In cases where the carboxyl group is involved in the deprotonation process, the absorption spectra were less affected (2−3% over a pH range of 2−11) and a conventional pH-metric method was used for the estimation of pK_a values instead. Solutions, 0.03−0.05 mM in concentration, were prepared in 50 mL of H_2O, containing 0.1 M KNO_3 to maintain a constant ionic strength. The initial pH of the solutions was adjusted to 11 by adding 0.2 M NaOH. The UV−visible absorption and emission spectra of each solution were obtained after adding acid and allowing the mixture to equilibrate. For the study of excited-state equilibrium, emission spectra acquired by exciting at one of the isosbestic points preserved over the entire pH excursion in the lowest-energy MLCT band. The spectral changes are completely reversible. The pK_a values are reported in Table 4.

Figure 3 shows the absorption changes upon addition of acid to alkaline solutions of $[(bpy)_2Ru(dpqOHCOOH)]^{2+}$ and $[(bpy)_2Ru(dpq(OH)_2)]^{2+}$. In the former, the lowest-energy MLCT band keeps its maximum at ∼455 nm while pronouncedly intensifying at around 430 nm (Figure 3a). To evaluate this observation, it should be recalled that the MLCT band is indeed an admixture of several singlet MLCT states.[27] Following protonation, these states may have been influenced quite differently. Considering the fact that the overall shapes of the MLCT absorption bands are all very similar, the increase in absorption value could be reminiscent of the increase in dipole moment of metal-to-dpq CT transition. The initial charge distribution, in the excited state of the deprotonated form, is now perturbed by the upcoming proton producing a larger transition dipole moment in the protonated form of the dpq.[28] However, due to the inherently broad nature of this band and overlapping of several MLCT states, the assignment of those unclearly resolved bands to each transition is not simple.

In this complex, the high-energy band at 330 nm in alkaline media is due to an intraligand $\pi-\pi^*$ transition within the anionic form of the dpq moiety and is not present either under acidic conditions or in nonaqueous solvents. Two isosbestic points are observed at 326 and 393 nm, while on the longer wavelength side of the MLCT band (>470 nm), the absorption intensity remains firm. The presence of isosbestic points verifies the existence of two *detectable* species in the equilibrium, most likely, the deprotonated and fully protonated forms. It is not possible to identify the monoprotonated species probably due to the similarity of its spectral features to those of the fully protonated species. Titration curves, obtained by plotting pH vs moles of acid added per mole of complex, shows the expected sigmoidal shape giving the first ground-state pK_{a1} value of 4.8 ± 0.2. The second ground- and two excited-state pK_a's (pK_{a2}, pK_{a1}*, and pK_{a2}* in Table 4) were determined from the relationship between absorption and emission intensities, respectively, with the pH.

The uncorrected emission spectrum has a maximum at 597 nm, which does not show an appreciable dependence on pH across 7 units (pH = 3−10). The emission intensity, however, increases with decreasing pH, which is consistent with the trend observed in emission lifetime data (Supporting Information, Figure 1S).

The 0.7 and 1.0 pK_a unit differences in the first and second sets of ground- and excited-state pK_a's indicate that the ligand electron density is higher in the excited state. Regardless of the overall ionic charge (2+ or 1+) of the complex, the electron transfer from metal to ligand, in this case dpqOHCOOH, redistributes more negative charge on the carboxyl and hydroxyl groups. The same conclusion has been reached in a number of structurally related Ru compounds.[29]

In $[(bpy)_2Ru(dpq(OH)_2)]^{2+}$, it must be noted that substitution of the carboxylic acid with a hydroxyl group yields a complex which has more detectable spectral changes, as a function of pH, in aqueous solution (Figure 3b and Table 4). Therefore, the ground- and excited-state pK_a's were all determined by spectrophotometric titration. As seen in Figure 3b, there are three isosbestic points observed at 334, 419, and 477 nm in acidic conditions. In alkaline media, the first two points shift to 337 and 417 nm, respectively, indicating the presence of a third species at higher values of pH, namely, the deprotonated form $[(bpy)_2Ru^{II}(dpqO_2^{2-})]$. In the absorption spectrum, a new intraligand $\pi-\pi^*$ band again appears at 350 nm with a shoulder at ∼370 nm. The lowest MLCT band first intensifies at its maximum but weakens along with its shoulder at 430 nm upon increasing the pH.

The emission from the acid form of this complex is at lower energy (uncorrected λ_{max} = 606 nm) and is more intense as compared with that observed from the basic form (λ_{max} = 594.5 nm, a plot for pH dependence of emission maximum is given in Supporting Information, Figure 2S). The emission intensities correlate well with the emission lifetimes. From this evidence, it can be postulated that in this case we are dealing with two closely located MLCT states representing two different excited-

(26) Turro, N. J. *Modern Molecular Photochemistry*; Benjamin Cummings: Menlo Park, CA, 1978.
(27) (a) Hager, C. D.; Crosby, G. A. *J. Am. Chem. Soc.* **1975**, *97*, 7031. (b) Sykora, M.; Kincaid, J. R. *Inorg. Chem.* **1995**, *34*, 3852.
(28) The same interpretation for a structurally similar ligand was given in Schoonover et al.: Schoonover, J. R.; Bates, W. D.; Meyer, T. J. *Inorg. Chem.* **1995**, *34*, 6421.
(29) (a) Zakeeruddin, S. M.; Nazeeruddin, M. K.; Humphry-Baker, R.; Grätzel, M.; Shklover, V. *Inorg. Chem.* **1998**, *37*, 5251. (b) Nazeeruddin, M. K.; Kalyanasundaram, K. *Inorg. Chem.* **1989**, *28*, 4251. (c) Shimidzu, T.; Izaki, K. *J. Phys. Chem.* **1985**, *89*, 642. (d) Lay, P. A.; Sasse, W. H. S. *Inorg. Chem.* **1984**, *23*, 4123. (e) Giordano, P. J.; Bock, C. R.; Wrighton, M. S.; Interrnate, L. V.; Williams, R. F. X. *J. Am. Chem. Soc.* **1977**, *99*, 3187. (f) Sun, H.; Hoffman, M. Z. *J. Phys. Chem.* **1993**, *97*, 5014.

Table 4. Ground- and Excited-State pK_a Values for Ru Complexes Determined by Means of Spectrophotometric Titration[a]

compound	[Ru]/M	pK_{a1}	pK_{a2}	pK_{a1}*	pK_{a2}*
$[(bpy)_2Ru(dpq(OH)_2)]^{2+}$	3.8×10^{-5}	6.0 ± 0.2	10.0 ± 0.2	6.5 ± 0.2	10.0 ± 0.2
$[(bpy)_2Ru(dpqOHCOOH)]^{2+}$	3.4×10^{-5}	4.8 ± 0.1[b]	6.4 ± 0.1	5.5 ± 0.2	7.4 ± 0.2
$[(bpy)_2Ru(dpq(COOH)_2)]^{2+}$	5.0×10^{-5}	3.5 ± 0.1[b]	6.6 ± 0.2[b]	3.9 ± 0.1	
$[(bpy)_2Ru(dppzc)]^{2+}$	1.0×10^{-5}	5.8 ± 0.2			

[a] At room temperature and in air-saturated solutions containing 0.1 M KNO_3. [b] Determined by conventional pH-metric method.

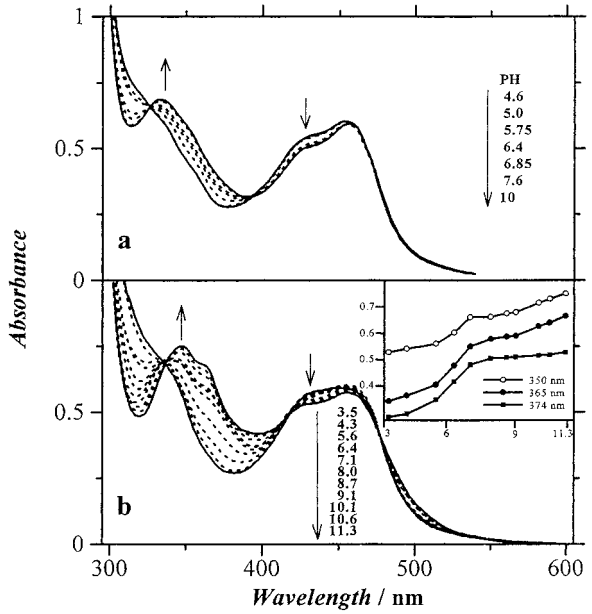

Figure 3. Absorption spectral changes of (a) (0.034 mM) $[(bpy)_2Ru(dpqOHCOOH)]^{2+}$ and (b) (0.050 mM) $[(bpy)_2Ru(dpq(OH)_2)]^{2+}$ as a function of pH in a 0.1 M KNO_3 aqueous solution. The inset in b shows the absorbance vs pH at 350 (open circle), 365 (filled circle) and 374 nm (filled rectangle).

state configurations that differ by their distribution of negative charge on different ligands. As previously mentioned, the first reduction potential in this complex could not be assigned to any of the bpy or dpq ligands (vide supra), indicating that these ligands may have LUMOs of the same energy level. It is most likely that, following the first deprotonation step, the dpq-localized MLCT is no longer the lowest and predominant emissive state. The increasing MLCT energy level, as a consequence of switching the lowest excited state from a dpq- to a bpy-localized one, narrows the energy gap between the MLCT and d−d states. In such cases, due to smaller activation energy, a faster surface-crossing rate can generally be expected.[18] This will eventually enhance the nonradiative decay rate leading to a lower quantum yield of emission. In addition, the finding of equal values for the second ground- and excited-state pK_a's (pK_{a2} = pK_{a2}* = 10.0 ± 0.2) strongly suggests that, in the monoprotonated form, the excited state is a bpy-localized MLCT configuration with almost no influence on the second deprotonation step of $dpq(OH)_2$. However, a 0.5-pK_a unit difference between the first ground- and excited-state pK_a's in this complex indicates that, in the protonated form, the lowest MLCT state is preferably localized on dpq. The interplay between selected MLCT excited states, distinguished by their distribution of charge on the ligand framework, is known to be an extremely complicated subject in the photophysics of polypyridyl metal complexes.[30]

In $[(bpy)_2Ru(dpq(COOH)_2)]^{2+}$, a plot of pH vs moles of acid added per mole of complex (Supporting Information, Figure 3S) shows two inflection points at pH 7.8 and 4.8 defining pK_{a2} = 6.6 ± 0.2 and pK_{a1} = 3.5 ± 0.1 for two protonation equilibria. The observation of two inflection points in this complex suggests that the carboxylic groups behave independently, leading to sequential dissociation processes. The uncorrected emission spectrum has a maximum at 598 nm in alkaline pH, which remains intact upon lowering the pH to 2. However, the emission intensity decreases with decreasing pH, which is due to the shorter lifetime of the acid form and is probably caused by proton-induced quenching. The spectrofluorometric titration gives a value of 3.9 ± 0.1 for the first excited-state pK_{a1}*, different from that of the ground state by 0.4 pH units. This demonstrates that once again the increased negative charge on the ligand will increase the base strength in the excited state.

In the case of $[(bpy)_2Ru(dppzc)]^{2+}$, considering the fact that this complex does not emit in aqueous solutions, only the ground-state pK_a (5.8 ± 0.2) was successfully determined.

It is interesting to compare the (first) ground-state pK_a's of $[(bpy)_2Ru(dcbpy)]^{2+}$,[29c] $[(bpy)_2Ru(dpq(COOH)_2)]^{2+}$, $[(bpy)_2Ru(dpqOHCOOH)]^{2+}$ and $[(bpy)_2Ru(dppzc)]^{2+}$, which are ~0.5, 3.5, 4.8, and 5.8, respectively. The differences in pK_a can be rationalized on the basis of both the donor/acceptor properties of the ligand and the electrostatic effect. As mentioned in the evaluation of the trend observed in oxidation potentials, at shorter distances, the ruthenium center reduces the electron density of the carboxyl moiety more efficiently, via either electrostatic interaction and/or π back-donation. There is also a good correlation between the oxidation potentials and the pK_a's of these complexes. The ruthenium oxidation potential in this series decreases in the order $[(bpy)_2Ru(dcbpy)]^{2+}$ > $[(bpy)_2Ru(dpq(COOH)_2)]^{2+}$ > $[(bpy)_2Ru(dpqOHCOOH)]^{2+}$ > $[(bpy)_2Ru(dppzc)]^{2+}$, which is anticipated to agree with the increasing order of the pK_a.

Transient Absorption Spectra. Transient absorption (TA) spectra for the ^{3}MLCT excited state of the Ru complexes are shown in Figure 4. In these spectra, bleaching of the MLCT band was observed with its maximum at ~460 nm. Upon the excitation and production of the Ru^{3+} ion core, the bpy-based intraligand $\pi-\pi^*$ transition was shifted to a lower energy (~310 nm) as an electrostatic effect of the highly charged metal ion.

In the TA spectrum of $[(bpy)_2Ru(dppzc)]^{2+}$, there are two sharp bands at 350 and 380 nm and a broad one (at 500−750 nm), all of which are attributed to the anion radical of the dppzc ligand (Figure 4a). The broad band could also be associated with LMCT transitions following the production of the Ru^{3+} ion core in the excited state. The presence of the second dppzc ligand, in $[(bpy)Ru(dppzc)_2]^{2+}$ (Figure 4b) and $[(phen)Ru(dppzc)_2]^{2+}$, does not introduce a significant change in the TA spectra of those complexes. However, addition of acid resulted in a decrease in their excited-state lifetimes to less than 1 ns in MeCN/10^{-2} M $HClO_4$ solution (acid was used to dissolve the samples). The shorter lifetimes in the presence of H^+ can be caused by interactions between the phenazine nitrogens and

(30) (a) Schoonover, J. R.; Bates, W. D.; Meyer, T. J. *Inorg. Chem.* **1995**, *34*, 6421. (b) Leasure, R. M.; Sacksteader, L. A.; Nesselrodt, D.; Reitz, G. A.; Demas, J. N.; DeGraff, B. A. *Inorg. Chem.* **1991**, *30*, 1330. (c) Giordono, P. J.; Fredricks, S. M.; Wrighton, M. S.; Morse, S. L. *J. Am. Chem. Soc.* **1978**, *100*, 2257.

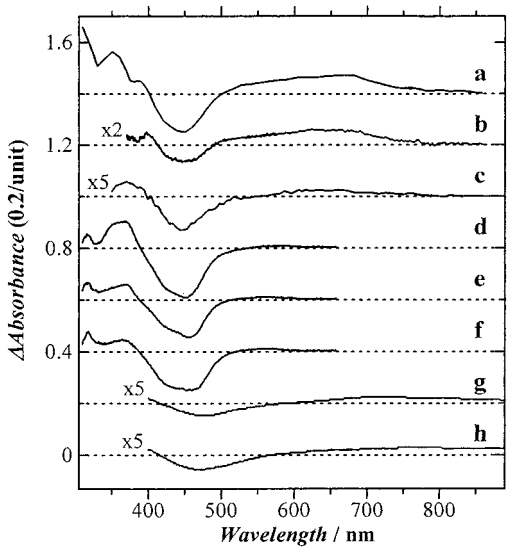

Figure 4. Room-temperature transient absorption spectra following 20 ns (532 nm) laser excitation of (a) $[(bpy)_2Ru(dppzc)]^{2+}$, (b) $[(bpy)Ru(dppzc)_2]^{2+}$ (in Ar-purged DMF), (c) $[(bpy)_2Ru(dpq(CN)_2)]^{2+}$, (d) $[(bpy)_2Ru(dpq(COOH)_2)]^{2+}$, (e) $[(bpy)_2Ru(dpqOHCOOH)]^{2+}$, and (f) $[(bpy)_2Ru(dpq(OH)_2)]^{2+}$, in Ar-purged MeCN; and 20 ps laser excitation of (g) $[(bpy)_2Ru(dpq(COOH)_2)]^{2+}/TiO_2$ and (h) $[(bpy)_2Ru(dpq(OH)_2)]^{2+}/TiO_2$, in air-saturated MeCN.

protons leading to quenching of the emission. Similar results have been reported for a series of dppz-containing Ru complexes, $[(phen)_nRu(dppz)_{3-n}]^{2+}$ ($n = 1, 2$).[30a,31]

In the excited states of dpq complexes, TA at ~360 nm could be assigned to a new $\pi-\pi^*$ transition within the anion radical of the corresponding dpq ligand (Figure 4c−f). A similar absorption band was also observed in alkaline solutions of $[(bpy)_2Ru(dpqOHCOOH)]^{2+}$ and $[(bpy)_2Ru(dpq(OH)_2)]^{2+}$. The relative intensity of this band, when compared to that of the band at 310 nm, is in the order $[(bpy)_2Ru(dpq(COOH)_2)]^{2+} > [(bpy)_2Ru(dpqOHCOOH)]^{2+} > [(bpy)_2Ru(dpq(OH)_2)]^{2+}$. This order neatly matches the dpq-ligand π-acceptor ability which itself is a function of the substitutions on dpq by the carboxylic acid and the hydroxyl group.

Comparing the two sets of TA in dppzc and dpq complexes, one distinguishable difference is the intensity of the positive band at longer wavelengths. This band is weakly detected in dpq complexes, with the more clearly observed one being in $[(bpy)_2Ru(dpq(CN)_2)]^{2+}$ (centered at 650 nm in Figure 4c). In the excited state of the dppzc complexes, the promoted electron can be expected to delocalize wider over the central phenazine part of the dppzc ligand introducing a larger dipole moment than the dpq ligand when compared to the ground state. Therefore, and as a result of increased extinction coefficient, more pronounced absorption intensities in dppzc complexes could be well correlated to a different amount of charge redistribution in the excited state of these systems.

The TA spectra for sensitized-TiO_2 electrodes (while dipped in air-saturated MeCN) showed a broad bleach from 420 to 570 nm and a positive absorption band from 600 to 900 nm which were promptly observed after the laser pulse (20 ps), indicating a rapid electron injection into TiO_2 and concomitant production of the oxidized dye (Figure 4g,h).[3] The most probable assignment for these bands is an overlap of the negative-ground-state bleaching and positive signal resulting from electron injection product, i.e., oxidized dye/e^- (TiO_2). The recovery of the TA,

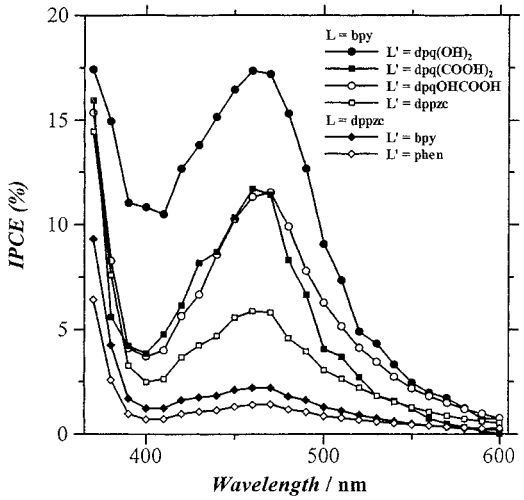

Figure 5. Plot of incident photon-to-current conversion efficiency (IPCE) as a function of excitation wavelength, λ, calculated from the expression $1240I_p/\lambda F$ where I_p is the photocurrent density in $\mu A/cm^2$ and F is photon flux in $\mu W/cm^2$. See text for experimental details.

which is attributed to electron tunneling from TiO_2 donor state(s) to the oxidized Ru^{III} core,[32] happens in less than 100 ps. Approximately 50% of the initial amplitude recovers within 60 ns; this could be due to the excited-state decay of those dye molecules that do not photoinject efficiently. In addition, there is also a possibility for multiphasic recombination kinetics which has previously been reported for $[Ru(dcbpy)_3]^{2+}$-sensitized TiO_2.[33] Furthermore, the sensitized-TiO_2 electrodes were subjected to time-correlated single-photon counting measurements. No stimulated emission from the excited state of the dye could be resolved in these experiments. We thus concluded that a rapid electron injection occurs within our time resolution (40 ps). Accordingly, the weak luminescence, observed on the nanosecond time scale for the sensitized electrodes, seems to be originated from the sites electronically uncoupled with the Ti 3d conduction band manifold.

Photovoltaic Features. Photocurrent measurements were performed on the TiO_2 electrodes sensitized with a monolayer of the metal complexes, and the corresponding photoaction spectra are shown in Figure 5. In this series of Ru complexes, the highest incident monochromatic photon-to-current conversion efficiency (IPCE) was obtained for $[(bpy)_2Ru(dpq(OH)_2)]^{2+}$ (17% at 460 nm). In this case, the $dpq(OH)_2$ ligand lacks a lower-lying π^* level when compared, for example, to $dpq(COOH)_2$. The higher value of IPCE could be interpreted in terms of (i) a decrease in the nonradiative decay rate caused by introducing an electron-donating group (OH) to the ligand which destabilizes the $d\sigma^*$ orbital and results in a wider $d\pi-d\sigma^*$ energy gap,[22] (ii) the larger driving force of the electron-transfer process, or (iii) better electronic coupling with the surface Ti^{4+} centers due to the fact that hydroxyl group is smaller in size and can be adsorbed deeper into the surface.[6c]

From the data presented here, it can be concluded that even small changes in the structure resulting from the introduction of different functional groups (used for grafting) can considerably improve the efficiency of photoconversion. Furthermore, strong binding of this type of inorganic sensitizer to the semiconductor surface and rapid electron injection, two critical

(31) Holmlin, R. E.; Yao, J. A.; Barton, J. K. *Inorg. Chem.* **1999**, *38*, 174.
(32) Ford, W. E.; Rodgers, M. A. *J. Phys. Chem.* **1994**, *98*, 3822.
(33) O'Regan, B.; Moser, J. E.; Anderson, M.; Gratzel, M. *J. Phys. Chem.* **1990**, *94*, 8720.

factors in the stability of solar cells, are both important features of our results.

Conclusion

A series of new Ru polypyridine complexes based on derivatives of fully conjugated and planar ligands dppz and dpq were prepared. Using a recently established synthetic route, those heteroaromatic entities were obtained by the reaction between $phenO_2$, coordinated to the ruthenium, and a diamino motif, containing either the desired or convertible functional groups for further application, i.e., grafting to the nanocrystalline TiO_2 surfaces. The ruthenium complexes were characterized with respect to their absorption, luminescence, and redox behavior together with other spectrometric method such as NMR and ESI-MS. Electrochemical data, transient absorption spectra, and finally determination of the ground- and excited-state pK_a's provided evidence for a charge transition from Ru to a particular ligand. With a combination of grafting functional groups, this ligand bridges the metal moiety to the acceptor site of the semiconductor forming a photochemically active donor−acceptor couple. The observation of a larger IPCE obtained in $[(bpy)_2Ru(dpq(OH)_2)]^{2+}$, utilizing a new mode for grafting, provides a model for structures necessary to design inorganic molecular dyes for photosensitization of nanocrystalline TiO_2.

Acknowledgment. We wish to thank the Japanese Ministry of International Trade and Industry for the financial support. B.G. gratefully acknowledges Japan Science and Technology Corporation (JST) for a research fellowship. Particular thanks are given to Professor Takeshi Ohno, for helpful discussion, and Dr. Koichi Nozaki and Dr. Akio Yoshimura, Photochemistry Lab, Osaka University, for their invaluable assistance in obtaining nano- and picosecond time-resolved transient absorption spectra, and time-correlated single-photon counting. We also acknowledge Mrs. Marlene Bell-Gholamkhas and Dr. Sean Simpson for their help in preparation of this manuscript.

Supporting Information Available: Plots showing pH dependence of emission lifetimes in dpq complexes, pH dependence of emission maximum and intensity for $[(bpy)_2Ru(dpq(OH)_2)]^{2+}$, conventional pH-metric result for $[(bpy)_2Ru(dpq(COOH)_2)]^{2+}$, and scheme for sequential deprotonation processes in selected complexes. This material is available free of charge via the Internet at http://pubs.acs.org.

IC0006605